Wasit Journal of Engineering Sciences

Journal homepage: https://ejuow.uowasit.edu.iq

Energy-Efficient Optimization of mm-Wave Communication Using a Novel Approach of Beamspace MIMO-NOMA

Ammar A. Majeed[1], Ismail Hburi[1]

Affiliations
Department of Electrical Engineering, Wasit University, Wasit, Iraq

Email:

1- ammara302@uowasit.edu.iq

2- isharhan@uowasit.edu.iq

Received
29-January-2022
Revised
29-March-2022
Accepted
17-April-2022
Doi: 10.31185/ejuow.Vol10.Iss2.287

Abstract:

The new concept of Beamspace Multiple Input Multiple Output system (BS-MIMO) was developed to address the issue of reduced Energy Efficiency (EE) of the traditional MIMO in millimeter-Wave (mm-Wave) wireless communication systems by decreasong the large number of radio frequency chains (RF-chains) while maintaining the same number of antennas in those systems. On the other hand, fewer RF-Chains leads to a smaller number of users that the system can serve as a result of the number of use rs that can be served must be equal to/or less than the RF-chains' number. To overcome the above issue, the BS-MIMO is proposed to be integrated with Non-Orthogonal Multiple-Access (NOMA) scheme to produce the novel approach of BS-MIMO-NOMA. As a result, the novel scheme is capable of serving a group of users with correlated channels via a single RF-chain. In this paper, we will address the issue of EE of the above-mentioned communication systems. Specifically, we propose and develop an iterative algorithm with a low complexity that achieves near-perfect performance. The proposed scheme, named MSE-DPA (for Mean-Square-Error-Based Dynamic Power Allocation Algorithm), is checked to ensure this validity of Figure-of-Merit. The simulation results indicate that the EE is approximately 85% greater than that of traditional (fully-digital) MIMO systems for a certain fair system and environment scenario.

Keywords: MIMO, mm-Wave, Beamspace, RF-Chain, NOMA. Beamspace-MIMO-NOMA, Energy Efficiency, Power Allocation, Performance optimization algorithms.

الخلاصة: لقد تم تطوير مفهوم قناة الإشعاع المكانّي للتغلب على مساوئ انخفاض كفاءة الطاقة في أنظمة متعددة الهوائيات التقليدية التي تعمل ضمن نطاق الموجات الميليمترية لأنظمة الاتصالات اللاسلكية. في هذه المنظومات يتم تقليل العدد الكبير لِـ سلاسل الترددات الراديوية مع المحافظة على نفس عدد الهوائيات المرتبطة بتلك الأنظمة. من جانب أخر، يؤدي عدد سلاسل الترددات الراديوية المنخفضة الى تقليل عدد المستخدمين الكلي الذين يتم خدمته بنفس الوقت/التردد داخل النظام نظراً لكون عدد المستخدمين يجب ان يكون دائما مساوٍ او اقل من عدد سلاسل الترددات الراديوية المستخدمة. مؤخراً، تم اقتراح دمج كل من مفهومي قناة الإشعاع المكانّي مع تقنية الوصول المتعدد غير المتعامد (لتكوين المفهوم الحديث BS-MIMO-NOMA) ونتيجة لذلك أصبح من الممكن خدمة أكثر من مستخدم ممن يمتلكون قنوات متداخلة غير مستقلة عبر سلسلة واحدة لمكونات التردد الراديوي. يتناول هذا البحث كفاءة الطاقة للنظام المقترح أعلاه. حيث تم اقتراح وتطوير خوارزمية تكرارية منخفضة التعقيد للحصول على أداء شبه مثالي. تم تسمية هذه الخوارزمية بخوارزمية توزيع الطاقة الديناميكية القائمة على متوسط الخطأ المربع (MSE-DPA اختصاراً). تظهر نتائج المحاكاة تفوقا واضحا للعمل المقترح من ناحية كفاءة الطاقة على بقية الأنظمة التقليدية حيث تم الحصول على ما يقارب ٨٥% كفاءة طاقة اعلى مقارنتاً بالنظام التقليدي لأنظمة متعددة الهوائيات وذلك لضروف عمل معينة متكافئة للحالتين.

1. INTRODUCTION

Modern wireless communications (5G and beyond) have a slew of requirements to achieve the expected and promising performance. These requirements include high-speed connectivity, massive capacity, extra data, increased reliability, increased bandwidth, and high data transfer rates [1]. Additionally, by employing mm-wave frequencies in the range of (30-300 GHz), additional antenna elements can be placed at the same physical size, enabling Massive MIMO (MA-MIMO) antennas [2]. The MA-MIMO provides both beamforming and spatial multiplexing gain as the main key features of this scheme. However, utilizing mm-wave MIMO techniques appears pointless because of high power consumption and hardware complexity [3]. The above drawbacks come from the fact that each antenna element in the MA-MIMO wireless communication system must be connected to electronic components known as RF-Chain; each of these chains consumes approximately 250mW [4]. Thus, the use of MA-MIMO results in a massive number of RF-Chains, resulting in the drawbacks mentioned earlier. According to previous research, RF-chains share up to 70% of total power consumption at the transmitter and receiver ends [5], or approximately 64W for our proposed scheme with 256 antennas. There are numerous strategies for reducing the RF-Chains' number in order to achieve the required EE while also reducing the system's complexity, such as phase shifter networks [6], complex gain combiners [7], beam selection [8], and antenna selection [9].

Recently, a new concept has been proposed to reduce the RF-chains known as Beamspace-MIMO (BS-MIMO), which is equipped with discrete lens-antenna arrays (DLA) to decrease the RF-Chains' number significantly [3]. Where the traditional spatial channel of MIMO can be converted to a beamspace channel via the use of BS-MIMO to take advantage of the sparsity of the mm-wave channel, there will be a significant reduction in the system's power consumption and interference due to the beamspace channel's selection of dominant beams [10], as shown in **Figure 1**. Additionally, BS-MIMO provides narrower beams than the traditional schemes of MIMO/ MA-MIMO using a lens antenna array, which reduces the power consumed by individual beams and inter-beam interference. That is why BS-MIMO achieves near-optimal performance with a significantly larger EE than regular MIMO and outperforms more typical beam selection algorithms [8].

To reduce the interferences between users of multiple beams, in contrast to previous research by other authors who employ zero-forcing Precoding (ZF). The proposed BS-MIMO-NOMA considers the Maximum Signal-to-Leakage plus-Noise Ratio algorithm, i.e., SLNR-MAX-beamforming, which balances in-between the zero-forcing and maximum ratio transmission where it maximizes the signal to leakage plus noise ratio. In this precoding scheme, the influences of noise are not neglected, and there are no limitations on the number of transmitting antennas in comparison with the zero-forcing Precoding, which amplifies the noise signal specifically for the channel that suffers a high level of attenuation, i.e., SLNR-MAX-beamforming eliminates the noise-amplification that created in Zero-Forcing. Also, we shed more light on the influence of different parameters on the performance of the proposed scheme.

The remainder of this article is organized as follows. Section 2 represents the theoretical background; section 3 lists the contributions of this paper; section 4 introduces the BS-MIMO and BS MIMO-NOMA system models; Section 5 discusses the data-rate problem formulation, and Section 6 illustrates the numerical and simulation analysis. Finally, section 7 introduces the paper's conclusion.

2. THRESHOLD BACKGROUND

BS-MIMO remained a viable and promising concept in 5G wireless communications and beyond until recently, when user equipment devices grew exponentially. This weakness is because beamspace suffers from a key disadvantage: the limited users' number who can be served at the identical time and frequency recourses, which should not be greater than the decreased RF-chains' number; this is because of the Degree of Freedom (DOF) created by RF-Chains should be greater than the DOF produced by users [11]. Additionally, another promising wireless communication approach for the fifth generation and beyond is the Non-Orthogonal Multiple-Access (NOMA) scheme, which is based on the principle of sharing the identical resources of time/frequency/code domain in the wireless communication systems; this allows several users to be served by the identical beam and hence, the same RF-Chain [12][13].

NOMA technique offers several benefits, such as making enormous connectivity, lower latency, and better quality of service (QoS) [14]. Thus, one of the most significant constraints in wireless communications is broken, which states that the number of user equipment terminals should not exceed the RF-Chains' number. It should be noted that the NOMA technique can be divided into several sub-techniques that use several aspects as multiple divisions, for instance, sparse-code multiple-access NOMA (SCMA-NOMA) in addition to pattern-division multiple-access NOMA (PDMA-NOMA) [15]. Also, power-division NOMA (PD-NOMA) uses the power domain multiplexing with the help of successive-interference-cancellation (SIC), i.e. it serves several users by a similar beam with identical time-frequency-space resources via the use of power allocation for each user [16].

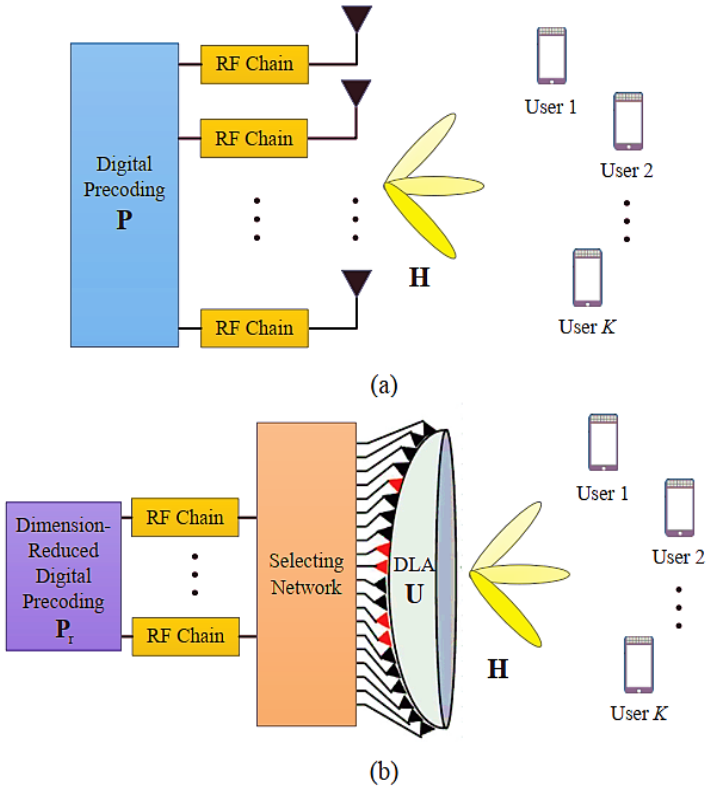

Figure 1. MIMO system architectures comparison:
(a) Conventional MIMO in the spatial domain; (b) The concept of BS-MIMO [10].

PD-NOMA has a significant increase of attention in recent years due to the possibility of its use in most areas of wireless communications, especially as it meets most of the requirements for 5G and the Internet of Things (IoT) wireless communication systems [17]. For this reason, several studies have been done to enhance the system's total performance. For example, authors in [18] proposed a dynamic power-allocation that customize power for each user to obtain both EE and Spectral Efficiency (SE) and reduce the interference of the inter-beam and intra-beam to achieve near-optimal performance. Figure 2 illustrates the taxonomy of various NOMA techniques [19]. Authors in [20] proposed a new approach that combines the benefits of the BS-MIMO concept with that of the NOMA technique to produce the BS-MIMO-NOMA. Numerous studies proposed multiple algorithms for achieving near-perfect SE performance while increasing EE and reducing computational and hardware complexity. The authors in [14] resort to the second-order cone trick and the sequential convex approximation to tackle the difficulty of the non-convexity of BS-MIMO-NOMA's power allocation problem. [21] Gray Wolf and Beetle Swarm optimization techniques are combined to maximize multiple performance criteria (SE and EE) in BS-MIMO-NOMA.

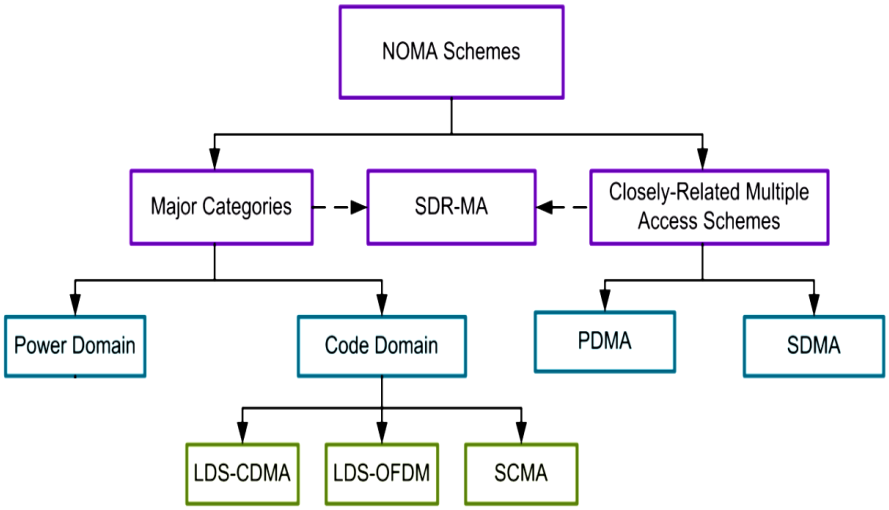

Figure 2. A straightforward categorization of NOMA techniques [19].

The authors of [22] used the Karush Kuhn Tucker conditions to derive a closed-form expression for the power allocation for different channel information (perfect and imperfect). The power allocation problem in MIMO-NOMA schemes is addressed in [23] using deep and non-deep learning techniques. To improve these systems' EE, multi-dimensional PA tasks that are non-linear programming (mixed-integer) problems were developed. To this end, the issue is first investigated using a non-deep learning technique, followed by a proposal for a shifting additional resources approach in two cases: variable and fixed inter-cluster power. After that, a machine learning (ML) scheme was suggested to eliminate the PA task.

3. CONTRIBUTIONS

In contrast to the work in [14], the mean square error technique in conjunction with the Woodbury inverse identity is used to eliminate the power allocation formula in this paper. As a result, the following contributions are summarized in this work:

- An energy-efficient dynamic power allocation algorithm for mm-wave BS-MIMO-NOMA is proposed. The formulation of the problem (non-convex fractional programming) considers the most important constraints for all users, namely a power budget and a minimum rate; an iterative algorithm is proposed to achieve the power allocation results.
- The proposed BS-MIMO algorithm performs both inter-beam and intra-beam power allocation tasks to increase data throughput while maintaining fairness and the total power of all users.
- The performance criteria for the system (EE) are validated using simulations for a variety of system parameters.

Notation: For matrix and vector representation, capital and small letters are used in bold, respectively. The symbol $[\text{-}]^{T}$ is used to represent the transpose of matrix, $[\text{-}]^{H}$ for complex-conjugate (Hermitian), $[\text{-}]^{-1}$ for matrix inversion, $[\text{-}]^{\dagger}$ for complex-conjugate of the transpose (Dagger). $\| \text{-} \|_{p}$ represents the norm operation with a length of p. Other matrix representations such as diagonal of matrix P denoted by using diag [p], expectation matrix denoted by E [-], identity Matrix of dimensions $\boldsymbol{NxN}$ denoted by I_N. $\boldsymbol{M}(\boldsymbol{l}, -)_{\boldsymbol{l} \in \boldsymbol{a}}$ denotes the sub-matrix of M that contains $\boldsymbol{l}$-th row of $\boldsymbol{M}$ where all $\boldsymbol{l} \in \boldsymbol{a}$. Finally, $|\boldsymbol{a}|$ represents the $\boldsymbol{a}$ set elements number.

4. SYSTEM MODEL

The downlink of a single-access point (AP) mm-wave wireless communication system is discussed in this article. The BS-MIMO system model will be reviewed first, and then the proposed BS-MIMO-NOMA scheme will be presented. Assume that the AP consists of *N* antenna elements connected by N_{RF} RF-Chains and serving *K* users, each with one antenna element. The block diagram of the proposed scheme is shown in Figure 3.

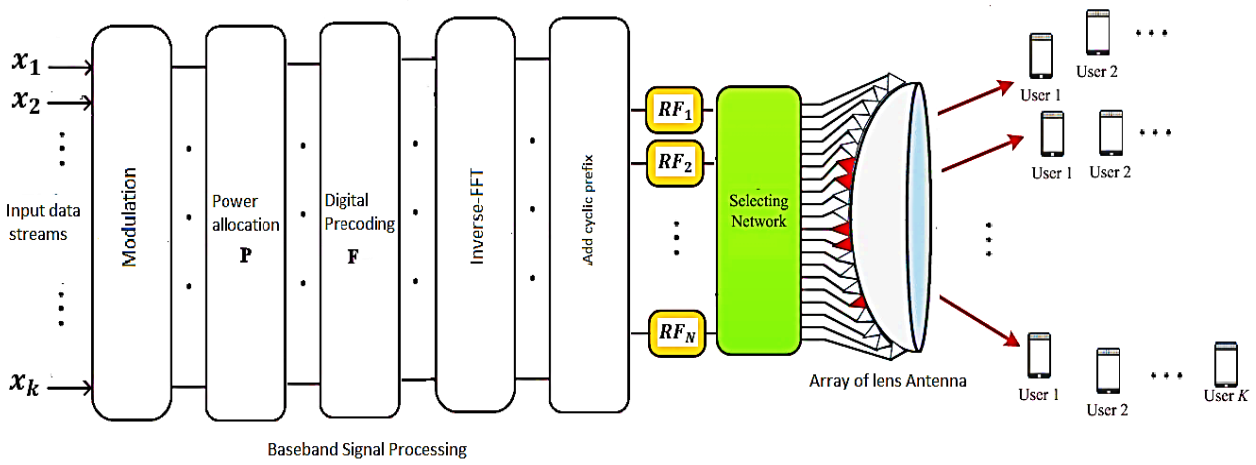

Figure 3. Block diagram for the proposed BS-MIMO-NOMA system.

By taking the conventional MIMO system as an example, consider the received signal vector $[y_1, y_2, \dots, y_K]^T$ may also be written as

$$\boldsymbol{y} = \boldsymbol{G^H F}.\boldsymbol{x} + \boldsymbol{n} \tag{1}$$

Where $\boldsymbol{G}$ is the channel matrix, $\boldsymbol{G} = [\boldsymbol{g}_1, \boldsymbol{g}_2, \dots, \boldsymbol{g}_K]$, $\boldsymbol{g}_k$ is the channel vector between the AP and *k*- th user, *F* is the beamforming matrix, $\boldsymbol{x} = \mathbf{Ps}$ is the vector of the transmitted signal, also, $\boldsymbol{x} = [\boldsymbol{x}_1, \boldsymbol{x}_2, \dots, \boldsymbol{x}_k]$ for all *K* users, and $\boldsymbol{n}$ is the Additive-White-Gaussian-Noise (AWGN). It is noteworthy that the channel model of Saleh-Valenzuela, which is the most widely used, has been adopted [3][8][20]. The Saleh-Valenzuela channel model is presented in more detail in the following sub-section

4.1. Saleh-Valenzuela Channel Model

Multipath propagation occurs when radio signals travel over two or more routes to reach the receiving antenna. Multipath is caused by air ducting, ionospheric reflection, and reflection from water and land features like mountains and buildings. Receiving the same signal over many paths can cause constructive or destructive interference and phase shifting between the receiving signal. Multipath propagation is now considered one of the most important parameters in 5G due to the low wavelengths of the communication signals [24].

The multipath propagation of the considered channel model was proposed for the first time in 1987 by A. Saleh and R. Valenzuela [25]. The authors used a 1.5 GHz communication frequency between two omnidirectional antennas within a mid-size building. They employed a unique measurement approach that relied on averaging the square-law-detected received pulse response while sweeping the transmitted pulse's frequency. Several results were obtained, the most important of which are: the channel formed inside the mentioned building is almost static, and its change is very slow over time. The maximum recorded time delay (latency) was about 200 nanoseconds. Also, in the case of non-Line of sight, the signal attenuation varied over a 60 dB range.

The Saleh Valenzuela model is the most often utilized method for simulating indoor multipath (indoor environment). This model incorporates the delayed receipt of signals caused by clusters. As a result, the numerous delayed received signals come in packets. The Poisson law determines the packet spacing and the signal spacing inside each packet. The amplitude of the delayed clusters decreases exponentially, as does the amplitude of the peaks inside

each cluster [25]. The Eq. (2) below illustrate the channel vector formula of each connection between the AP and *k*- th user,

$$\boldsymbol{g_k} = \beta_k^{(0)}\, \boldsymbol{a}\left(\theta_k^{(0)}\right), + \sum_{l=1}^{L} \beta_k^{(l)}\, \boldsymbol{a}\left(\theta_k^{(l)}\right) \tag{2}$$

where the Line-of-Sight (LoS) of the *k*- th user is represented by $\beta_k^{(0)}\, \boldsymbol{a}\left(\theta_k^{(0)}\right)$, in which $\beta_k^{(0)}$ implies the complex gain, and $\boldsymbol{a}\left(\theta_k^{(0)}\right)$ refers to the spatial direction. The L indicates the total number of Non-Line-of-Sight (NLoS) components is represented by $\sum_{l=1}^{L} \beta_k^{(1)}\, \boldsymbol{a}\left(\theta_k^{(1)}\right)$ for $1 \le l \le L$ is the *l*-th NLoS components of the *k*-th user.

4.2.System Model of BS-MIMO

The RF-Chains number is similar to the antenna elements number in the BS. Yields, $N_{RF} = N$, which is a vast RF-Chains number (about 256 antenna elements) when mm-wave large-scale MIMO systems are used [10]. That is why the use of mm-wave large-scale MIMO in practical systems is pointless due to its high cost and power consumption and the undesirable complexity introduced by a large number of RF-Chain [8]. As mentioned previously, each RF-Chain consumes approximately 250mW; therefore, for a system with 256 antenna elements, the Rf-Chain consumes approximately 64W, which is not a negligible power to loss [4]. The BS-MIMO concept is introduced to address this issue by utilizing a lens-antenna array to reduce the number of RF chains without sacrificing system performance. As a result, the MIMO spatial domain is transferred to the beamspace channel [26].

The BS-MIMO received signal vector $\bar{y}$ is expressed as follows,

$$\bar{\boldsymbol{y}} = \boldsymbol{G}^H\, \boldsymbol{D}^H\, \boldsymbol{F}.\boldsymbol{x} + \boldsymbol{n} \;=\; \bar{\boldsymbol{G}}^H\, \boldsymbol{F}\, \boldsymbol{x} + \boldsymbol{n} \tag{3}$$

where, $\bar{\boldsymbol{G}}^H$ is the channel matrix of bemaspace, and it is expressed as,

$$\bar{\boldsymbol{G}} = \boldsymbol{DG} = [\bar{\boldsymbol{g}}_{\boldsymbol{1}}, \bar{\boldsymbol{g}}_{\boldsymbol{2}}, \dots, \bar{\boldsymbol{g}}_{\boldsymbol{K}}], \tag{4}$$

where the vector $\bar{\boldsymbol{g}}_K = \boldsymbol{D}\boldsymbol{g}_K$ is the BS-MIMO channel between the AP and k-th user, and $\boldsymbol{D}$ provides the steering vectors of the lens-antennas (the array of B- beams (orthogonal directions) that overlay the whole angle space [27]. Hence, $\boldsymbol{g}_k$ in Eq. (2) is the vector of the spatial channel that fourier-transformed to $\bar{\boldsymbol{g}}_k$. Now, each row of the beamspace channel matrix $\bar{\boldsymbol{G}}$ denotes a single beam transmitted between transmitter and receiver. Similarly, all rows of $\bar{\boldsymbol{G}}$ are spatially directed B beams $\theta_1, \theta_2 \dots, \theta_B$. As a result, as is well known, the number of prevalent scatters in mm-wave communication channels is quite small. Consequently, the number of NLoS paths L is less than beams B. As a result, the channel matrix of beamspace $\bar{\boldsymbol{G}}$ can be asserted to exhibits a sparse behaviour, as the number of prevalent elements in each vector of beamspace channel $\bar{\boldsymbol{g}}_k$ is significantly less than the number of beams B. Therefore, due to the above reason, we can assert that the channel matrix of beamspace $\bar{\boldsymbol{G}}$ exhibits a sparse behaviour [26]. Hence, a BS-MIMO scheme with significantly reduced dimensions can be designed with near-optimal performance because of this sparsity behaviour. As previously stated, the beamspace fundamental limit is $N_{RF} \ge K$, which means that the number of RF-Chains must be equal to or greater than the number of users served in the same time-frequency resources since the DoF provided by RF-Chains should be greater than -or at least equal to - the DoF required by users [3][8] [10][26], to overcome this limit, a novel approach has been proposed that emerged the NOMA technique with the concept of BS-MIMO [28], as detailed in the following subsection.

4.3. System Model of BS-MIMO-NOMA

To overcome the limitations mentioned above of BS-MIMO, the BS-MIMO-NOMA has been proposed, which can concurrently serve multiple users by exploiting the same resources (time, frequency, and spatial domain). It is worth noting that multiple users can be selected within the same beam; these users share correlated channels. Consequently, multiple beam section methodologies have been devised to determine the optimal user for each beam and hence for each RF-Chain. For example, in [8], Optimizing the signal-to-interference-plus-noise (SNIR) approach is advised. Additionally, [27] introduces the Maximum-Magnitude approach. According to the authors in [10], the

probability of users having a correlated channel (choosing the same beam) is approximately 87% in a conventional architecture of mm-wave communication with 256 antenna elements and 32 user equipment.

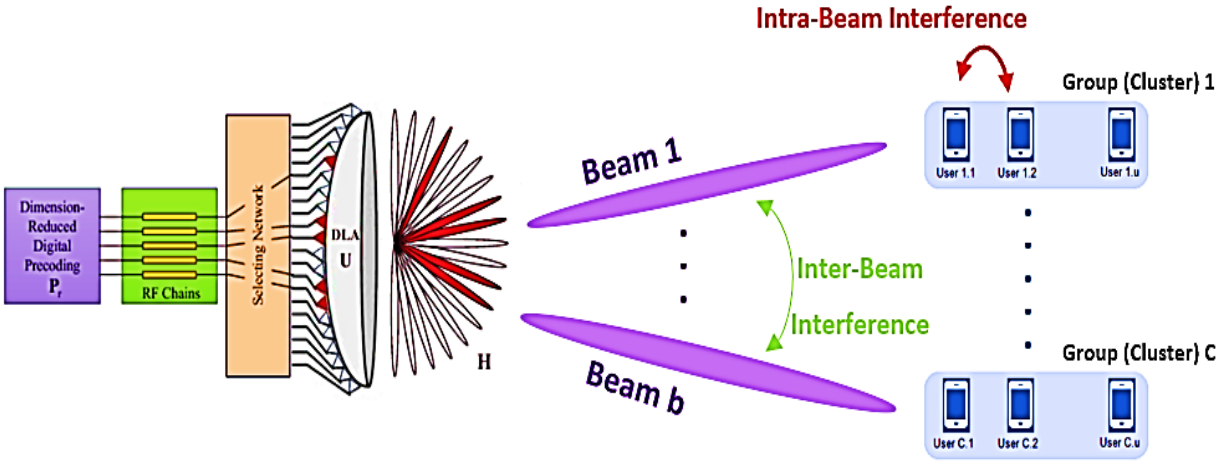

Figure 4. BS-MIMO-NOMA system model.

In contrast to BS-MIMO, which requires the system to select a single user for each RF-Chain, the BS-MIMO-NOMA can simultaneously serve all correlated users utilizing a single beam and a single RF-Chain. This feature results in the number of served users being higher than the number of RF-Chains, i.e., $N_{RF} \leq K$, which is a key feature of BS-MIMO-NOMA [28]. As mentioned before, the above scheme uses the same time, frequency, and spatial domains for all users serviced concurrently by the same beam\RF-Chain. Thus, the multiplexing is dependent on each user's power allotment within the group of conflicting users [18]. Figure above illustrates the concept of operation of the BS-MIMO-NOMA approach. The received signal of the BS-MIMO-NOMA system approach, which will be shown in Figure below, can be expressed as,

$$y_{kb} = \underbrace{\bar{\boldsymbol{g}}_{kb}^{H}\, \boldsymbol{f}_{kb} \sqrt{P_{kb}}\, X_{kb}}_{Useful\ Signal} + \underbrace{\bar{\boldsymbol{g}}_{kb}^{H}\, \boldsymbol{f}_{kb} \sum_{k \in K} \sqrt{P}\, X_{kb}}_{intra-beam\ interferences} + \underbrace{\bar{\boldsymbol{g}}_{kb}^{H} \sum_{\substack{i \in B \\ i \neq b}} \sum_{k \in |K|} \boldsymbol{f}_{kb} \sqrt{P_{ki}}\, X_{ki}}_{inter-beam\ interferences} + \underbrace{n_{kb}}_{AWGN} \tag{5}$$

Where y_{kb} is the received signal of the k-th user from the b-th beam, $\bar{\boldsymbol{g}}_{kb}^{H}$is the beamspace channel vector, $\boldsymbol{F}_{b}$is the beamforming matrix. The first part of (5) refers to the useful signal arrived to the k-th user. The second part represents interference between users who share a beam. The third part is concerned with interference between users on different and neighboring beams. The last part corresponds to AWGN. $\sqrt{P_{kb}}$ is the power received to the desired user, X_{kb} is the information signal received to the user, lastly, $\boldsymbol{f}_{kb}$ refers to the beamforming vectors, which should have a precise-designed to suppress the inter-beam interference. The authors in [12] considered the possibility of removing intra-beam interference by the use of SIC. Due to the superposition in NOMA, which causes this type of interference. Despite this, users are also affected by interference from the other beams. As a result, the suggested BS-MIMO-NOMA approach is anticipated to be ineffective and unstable in practice without precise beamforming and power allocation to increase the total data rate, SINR and reduce interference. Hence, back to (5), the SINR of the above scheme can be represented as follows [18],

$$\Gamma_{kb} = \frac{P_{kP} \| \bar{\boldsymbol{g}}_{\mathrm{kb}}^{H}\, \boldsymbol{f}_{kb} \|_{2}^{2}}{I_{intra-beam} + I_{inter-beam} + n_{kb}^{2}} \tag{6}$$

where, Γ_{kb} refers to SINR of the k-th user in the b-th beam, $\| \bar{\boldsymbol{g}}_{\mathrm{kb}}^{H}\, \boldsymbol{f}_{kb} \|_{2}^{2}$ corresponds to the direct beamspace channel gain. The terms of the denominator of this equation can be represented as follows,

$$I_{intra-beam} = \| \bar{\boldsymbol{g}}_{\mathrm{kb}}^{H}\, \boldsymbol{f}_{kb} \|_{2}^{2} \sum_{k \in K} P_{kb} \tag{7}$$

$$I_{inter-beam} = \sum_{i \neq b} \sum_{k \in |K|} \| \bar{\boldsymbol{g}}_{kb}^{H} \boldsymbol{f}_{kb} \|^2 \; P_{ki} \tag{8}$$

where P_{ki} stands for the power of the k-th user in the i-th beam. Consequently, the data rate of the *k-th* user in the *b-th* beam can be calculated using this formula,

$$R_{kb} = \ln(1 + \Gamma_{kb}) \tag{9}$$

where, R_{kb}, the data rate of the *k-th* user in the *b-th* beam. Now, the overall data sum rate for the proposed approach of the non-orthogonal-multiple-access BS-MIMO is represented as follows,

$$R_{sum-rate} = \sum_{i \in |b|} \sum_{k \in |K|} \ln(1 + \Gamma_{ki}) \quad nats/sec/Hz \tag{10}$$

5. DATA RATE PROBLEM FORMULATION

Unlike in typical beamspace-MIMO, where each RF-Chain serves only one user, any linear beamforming approach such as zero-forcing (channel pseudo-inverse) can be used as a beamformer to eliminate inter-beam interference because of $N_{RF} \geq K$. On the other hand, the classical ZF approach cannot be used in the proposed BS-MIMO-NOMA scheme due to K $\geq N_{RF}$, This means that pseudo-matrix inversion of the beamspace channel cannot be used here due to the number of users being bigger than the number of antennas. As per our previous discussion, In our study, we employed a significant type of linear Precoding, i.e., the SLNR-MAX-beamforming [29], which is shown to be very useful for 5G technologies such as massive MIMO communication systems to null the multiuser interference and leads to a notable gain in quality with almost the same computation time of the common used ZF beamforming while has an easy analytical formula,

$$\boldsymbol{F} = (\bar{\boldsymbol{G}}\bar{\boldsymbol{G}}^{H} + \boldsymbol{n^2 I})^{-1} \tag{11}$$

Where it is clear from this formula that the SLNR-MAX-beamforming accounts for both the interference and noise levels. Additionally, power allocation must be optimized for different users in different beams to achieve the highest possible data sum rate of a given system. As discussed previously, the MIMO-NOMA technique is based on sharing the same time, frequency, and spatial domains to serve multiple users simultaneously utilizing the same beam. Hence, power allocation for the same beam and multiple users plays a critical role in reducing inter-beam interference and also enhances the overall data rate of the system. Therefore, many studies have been discussed to investigate the power allocation of MIMO-NOMA [13][18]. However, such a MIMO-NOMA approach uses near-perfect User-channel information, which is especially important in dense user scenarios when several users' equipment (UE) may be in the same beam. As a result, several users share the same geographical characteristics of the link line of sight (channel direction), which can weaken the users' clustering process, which is necessary for our approach to operate in a practical manner. The formula of optimizing the power-allocation can be written as,

$$\max_{P_{kb}} \quad \sum_{b \in |b|} \sum_{k \in |K|} \ln(1 + \Gamma_{kb}) \tag{12}$$

Subject to:

$$C1: \quad \ln(1 + \Gamma_{kb}) \geq R_{th}$$

$$C2: \quad \sum_{b \in B} \sum_{k \in |K|} P_{kb} \leq P_t$$

where, Γ_{kb} refers to SINR, R_{th} stands for the minimum amount of data rate that each user should have, or in other words, it represents the QoS to confirm the user's fairness performance, P_t corresponds to the total power transmitted by the whole system. Since the inequalities of the constraints are non-linear, in addition, the optimization problem objective is a non-convex function, so this task is an NP-hard problem due to the coupled parameters in the main objective and constraints expressions, see, for example, [30] and [31] for more details and proof of NP-hardness. It is worth noting that the objective of optimizing the sum performance is nondeterministic polynomial even in single-antenna wireless systems. Therefore, practical or feasible approaches have to be developed with affordable calculation

complexity algorithms and suboptimal solutions that achieve an adequate result. To this end, the first constraint (C1) is simplified, i.e., put it as a linear-inequality with the aid of the inverse of the natural logarithm; this equation can be re-written using (6) and (9) as follows,

$$\bar{C}_1: \frac{P_{kP}\|\bar{\boldsymbol{g}}_{kb}^H \boldsymbol{f}_{kb}\|_2^2}{\|\bar{\boldsymbol{g}}_{kb}^H \boldsymbol{f}_{kb}\|_2^2 \ \sum_{k\in K} P_{kb} + \sum_{i\neq b} \ \sum_{k\in|K|} \|\ \bar{\boldsymbol{g}}_{kb}^H \boldsymbol{f}_{ki}\|^2 \ P_{ki} + n_{kb}^2} + 1 \geq 2^{R_{th}}$$

The joint interference term yields the problem in Eq. (12) to be linked via all users of each beam. Additionally, the individual power constraint results in the problem being connected via all beams. Constraints and objective tasks are polynomial in nature, i.e., they have a rational fraction with a non-convex structure. A minimum-mean-square-error (MMSE) algorithm is assumed to be used for receiving and detection. The MSE distance between the vector of transmitted data and the vector of received data decreases. To this end, the equalization coefficients are chosen to correspond to the channel characteristics (in our scenario, beamspace channel characteristics), such that,

$$W_{kb}{}^* = \arg\min_{W_{kb}} E\{|x_{kb} - W_{kb}\, y_{kb}|^2\} \tag{13}$$

where $E\{|x_{kb} - W_{kb}\, y_{kb}|^2$ is the MSE, $W_{kb}{}^*$ is the equalizer's optimal coefficients, and y_{kb} refers to the received signal. According to the above, the optimum coefficients of equalization in (13) can be re-written as follows, refer to Eq. (7), (8) and (13),

$$W_{kb}^* = \arg\min_{W_{kb}} \ (\ 1 - 2Rel\ \{\ W_{kb}\ \sqrt{p_{kb}}\ \ \bar{\boldsymbol{g}}_{kb}^H \boldsymbol{f}_{kb}\ \} + |W_{kb}|^2\ [\ p_{kb}\ .\ \|\bar{\boldsymbol{g}}_{kb}^H .\boldsymbol{f}_{kb}\|_2^2 + \ I_{kb} + \ n_{kb}{}^2\ ]\ ) = \arg\min_{W_{kb}} \{\ MSE_{kb}\ \} \tag{14}$$

where,

$$I_{kb} = \ \|\bar{\boldsymbol{g}}_{kb}^H \boldsymbol{f}_{kb}\|_2^2 \ \sum_{k\in K} P_{kb} + \sum_{i\neq b} \sum_{k\in|K|} \|\ \bar{\boldsymbol{g}}_{kb}^H \boldsymbol{f}_{ki}\|^2 \ P_{ki},$$

$Rel\{.\}$ stands for the complex number's real part. Thereby, for the last (14), a closed-form expression for the optimal equalization's coefficients can be signified with the aid of partial derivatives as described in **PROOF** below and be presented as follows,

$$W_{kb}^* = \left\{\ p_{kb}\ \|\bar{\boldsymbol{g}}_{kb}^H \boldsymbol{f}_{kb}\|_2^2 + \ I_{kb} + \ n_{kb}{}^2\ \right\}^{-1} \{\sqrt{p_{kb}}\ \bar{\boldsymbol{g}}_{kb}^H \boldsymbol{f}_{kb}\}^H \tag{15}$$

Now, by substituting W_{kb}^* in (14) with respect to (15), that leads to the following expression,

$$MMSE_{kb} = 1 - \ p_{kb}\ .\|\bar{\boldsymbol{g}}_{kb}^H .\boldsymbol{f}_{kb}\|_2^2\ (\ p_{kb}\ .\|\bar{\boldsymbol{g}}_{kb}^H .\boldsymbol{f}_{kb}\|_2^2 + \ I_{kb} + \ n_{kb}^2\ )^{-1} \tag{16}$$

5.1 Proof of the Mean Square Error Formula in eq. (16):

The mean of the square for the Euclidean distance of the error signal can be written as follows,

$$E\{|x_{kb} - W_{kb}\, y_{kb}|^2\} = \ (x_{kb} - W_{kb}\, y_{kb})^H\ (x_{kb} - W_{kb}\, y_{kb})$$

$$= \ x_{kb}{}^H\, x_{kb} \ + \ W_{kb}{}^2\, y_{kb}{}^H\, y_{kb} \ - \ 2W_{kb}\, Rel\{x_{kb}{}^H\ y_{kb}\} \quad \ldots(16.1)$$

Next, since we have a fixed unity power for both transmit and receive samples, i.e.,

$x_{kb}{}^H\, x_{kb} = \ y_{kb}{}^H\, y_{kb} \ = 1,$

this fact returns the following,

$$E\{|x_{kb} - W_{kb}\, y_{kb}|^2\} \ = \ 1 + \ W_{kb}{}^2 \ - \ 2W_{kb}\, Rel\{x_{kb}{}^H\ y_{kb}\} \quad \ldots(16.2)$$

Now, according to equations 5,7 and 8, we have,

$$y_{kb} = \underbrace{\sqrt{p_{kb}}\, \bar{\boldsymbol{g}}_{\mathrm{kb}}^{H}\, \boldsymbol{f}_{kb}\; x_{kb}}_{useful\ information} + interference_{\mathrm{signal}} + \mathrm{noise}_{\mathrm{signal}} ,$$

$$I_{intra-beam} = \left\| \bar{\boldsymbol{g}}_{\mathrm{kb}}^{H}\, \boldsymbol{f}_{kb} \right\|_2^2 \; \sum_{k \in K} P p_{kb} \quad , \; and,$$

$$I_{inter-beam} = \sum_{i \neq b} \sum_{k \in |K|} \| \bar{\boldsymbol{g}}_{\mathrm{kb}}^{H}\, \boldsymbol{f}_{ki} \|^2 \; p_{ki} \; .$$

Therefore, MSE becomes as follows,

$$E\{|x_{kb} - W_{kb}\, y_{kb}|^2\}$$

$$= 1 - 2\, Rel\{W_{kb} \left(\sqrt{p_{kb}}\, \bar{\boldsymbol{g}}_{\mathrm{kb}}^{H}\, \boldsymbol{f}_{kb}\right)\} + |W_{kb}|^2 \left(p_{kb} \left\| \bar{\boldsymbol{g}}_{\mathrm{kb}}^{H}\, \boldsymbol{f}_{kb} \right\|_2^2\right) + |W_{kb}|^2\, I_{kb} + |W_{kb}|^2\, n_{kb}{}^2 \quad \ldots (16.3)$$

Finally, this equation can be partially derived with respect to the value of the equalization coefficients to attain closed-form expression for the optimal value for this parameter, i.e., for optimal value $W_{kb}{}^{*}$. We have the following identity,

$$\frac{\partial E\{|x_{kb} - W_{kb}\, y_{kb}|^2\}}{\partial W_{kb}}$$

$$= \frac{\partial\{1 - 2\, Rel\{W_{kb} \left(\sqrt{p_{kb}}\, \bar{\boldsymbol{g}}_{\mathrm{kb}}^{H}\, \boldsymbol{f}_{kb}\right)\} + |W_{kb}|^2 \left(p_{kb} \left\| \bar{\boldsymbol{g}}_{\mathrm{kb}}^{H}\, \boldsymbol{f}_{kb} \right\|_2^2\right) + |W_{kb}|^2\, I_{kb} + |W_{kb}|^2\, n_{kb}{}^2\}}{\partial W_{kb}}$$

$$= \frac{\partial \left\{ \left|1 - W_{kb} \left(\sqrt{p_{kb}}\, \bar{\boldsymbol{g}}_{\mathrm{kb}}^{H}\, \boldsymbol{f}_{kb}\right)\right|^2 + |W_{kb}|^2 \left(p_{kb} \left\| \bar{\boldsymbol{g}}_{\mathrm{kb}}^{H}\, \boldsymbol{f}_{kb} \right\|_2^2\right) + |W_{kb}|^2\, I_{kb} + |W_{kb}|^2\, n_{kb}{}^2 \right\}}{\partial W_{kb}}$$

$$= 0 \; ,$$

which yields in the following,

$$0 - \sqrt{p_{kb}}\, \bar{\boldsymbol{g}}_{\mathrm{kb}}^{H}\, \boldsymbol{f}_{kb} + (W_{kb}{}^{*})^{H} \left(p_{kb} \left\| \bar{\boldsymbol{g}}_{\mathrm{kb}}^{H}\, \boldsymbol{f}_{kb} \right\|_2^2\right) + (W_{kb}{}^{*})^{H}\, I_{kb} + (W_{kb}{}^{*})^{H}\, n_{kb} = 0 \qquad \ldots (16.4)$$

Which in turns yields,

$$W_{kb}{}^{*} = \left\{ p_{kb} \left\| \bar{\boldsymbol{g}}_{\mathrm{kb}}^{H}\, \boldsymbol{f}_{kb} \right\|_2^2 + I_{kb} + n_{kb}{}^2 \right\}^{-1} \{\sqrt{p_{kb}}\, \bar{\boldsymbol{g}}_{\mathrm{kb}}^{H}\, \boldsymbol{f}_{kb}\}^{H} \qquad \ldots (16.5)$$

Consequently, substitute for the optimal coefficients from eq. (16.5) back in the MSE formula of eq. (16.3), the minimum mean square error will be as follows,

$$MMSE_{kb} = \min_{W_{kb}} \left(E\{|x_{kb} - W_{kb}\, y_{kb}|^2\}\right)$$

$$= \left|1 - 2\, Rel\{W_{kb} \left(\sqrt{p_{kb}}\, \bar{\boldsymbol{g}}_{\mathrm{kb}}^{H}\, \boldsymbol{f}_{kb}\right)\} + |W_{kb}|^2 \left(p_{kb} \left\| \bar{\boldsymbol{g}}_{\mathrm{kb}}^{H}\, \boldsymbol{f}_{kb} \right\|_2^2\right) + |W_{kb}|^2\, I_{kb} + |W_{kb}|^2\, n_{kb}{}^2 \right|_{W_{kb}{}^{*}}$$

$$= \left| \left|1 - W_{kb} \left(\sqrt{p_{kb}}\, \bar{\boldsymbol{g}}_{\mathrm{kb}}^{H}\, \boldsymbol{f}_{kb}\right)\right|^2 + |W_{kb}|^2 \left(p_{kb} \left\| \bar{\boldsymbol{g}}_{\mathrm{kb}}^{H}\, \boldsymbol{f}_{kb} \right\|_2^2\right) + |W_{kb}|^2\, I_{kb} + |W_{kb}|^2\, n_{kb}{}^2 \right|_{W_{kb}{}^{*}}$$

Hence, the minimum mean square error of the k-th user in the b-th beam ($MMSE_{kb}$) can be represented as,

$$MMSE_{kb} = 1 - p_{kb} \cdot \| \bar{\boldsymbol{g}}_{kb}^{H} \cdot \boldsymbol{f}_{kb} \|_2^2 \left(p_{kb} \cdot \| \bar{\boldsymbol{g}}_{kb}^{H} \cdot \boldsymbol{f}_{kb} \|_2^2 + I_{kb} + n_{kb}^2 \right)^{-1} \qquad \ldots (16.6)$$

The Woodbury inverse identity is employed [18], [32] to get,

$$(1 + \Gamma_{kb})^{-1} = 1 - p_{kb} \cdot \| \bar{\boldsymbol{g}}_{kb}^{H} \cdot \boldsymbol{f}_{kb} \|_2^2 \left(p_{kb} \cdot \| \bar{\boldsymbol{g}}_{kb}^{H} \cdot \boldsymbol{f}_{kb} \|_2^2 + I_{kb} + n_{kb}^2 \right)^{-1} \qquad (17)$$

5.2 Derivation Of The Sherman Morrison_ Woodbury's Formula:

The Sherman Morrison linear algebra formula, termed after J. Sherman and W. Morrison, can be used to do the inverse operation for a sum of the outer product of two vectors (u and v) and an invertible matrix X. The statement of this formula is as follows [33], [34]; If we have two column vectors (u and v) belong to $\mathbb{R}^n$, and an invertible matrix X belong to $\mathbb{R}^{(n\times n)}$ in this case, the matrix $(X + uv^T)$ can be averted in one case only, i.e., when $1 + v^T X^{-1} u \neq 0$. If this condition is satisfied, the results of the inverse will be determined as follows,

$$(X + uv^T)^{-1} = X^{-1} + \frac{X uv^T X^{-1}}{1+v^T X^{-1} u} \quad \dots (17.1)$$

Formula proof, let

$$Z = X + uv^T, \ and \ \ Y = X^{-1} + \frac{X^{-1} uv^T X^{-1}}{1+v^T X^{-1} u} \quad \dots (17.2)$$

Then for the formula to be correct, we have the following identity,

$$ZY = YZ = I \quad \dots (17.3)$$

First, we are going to verify $ZY = I$,

$$ZY = (X + uv^T)\left(X^{-1} + \frac{X^{-1} uv^T X^{-1}}{1 + v^T X^{-1} u} \right)$$

$$= X X^{-1} + uv^T X^{-1} - \frac{X X^{-1} uv^T A^{-1} + uv^T X^{-1} uv^T X^{-1}}{1 + v^T X^{-1} u}$$

$$= I + uv^T X^{-1} - \frac{u(1+v^T X^{-1} u)v^T X^{-1}}{1+v^T X^{-1} u} = I + uv^T X^{-1} - uv^T X^{-1} = I \quad \dots (17.4)$$

Next, to verify that $YZ = I$, one can leverage the same procedure to show that,

$$YZ = \left(X^{-1} + \frac{X^{-1} uv^T X^{-1}}{1 + v^T X^{-1} u} \right)(X + uv^T) = I \quad \dots (17.5)$$

Otherwise, if the non-zero condition is not valid, i.e., $1 + v^T A^{-1} u = 0$, in this case, from the lemma of matrix determinant, we have,

$dete.(X + uv^T) = (1 + v^T X^{-1} u)\, dete.(X) = 0$, and therefore, $X^{-1} = \frac{adj.(X)}{dete.(X)}$ does not exist.

A general statement for this expression is Sherman Morrison_ Woodbury's formula, where for a matrix U of dim. $(n \times k)$, and a matrix V of dim. $(k \times n)$, with $I + V X^{-1} U$ is invertible yields,

$$(X + UV)^{-1} = X^{-1} + X^{-1}U (I + V X^{-1} U)^{-1} VX^{-1} \quad \dots (17.6)$$

And for the current case, let $X = 1$, and $\Gamma_{kb} = UV$, such that;

$\boldsymbol{U} = P_{kP} \|\bar{\boldsymbol{g}}_{kb}^H \boldsymbol{f}_{kb}\|_2^2$ and $V = \frac{1}{\|\bar{\boldsymbol{g}}_{kb}^H \boldsymbol{f}_{kb}\|_2^2 \ \sum_{k\in K} P_{kb} + \sum_{i\neq b} \ \sum_{k\in |K|} \|\bar{\boldsymbol{g}}_{kb}^H \boldsymbol{f}_{ki}\|^2 P_{ki} + n_{kb}^2}$, where according to equations (6, 7 and 8), we have;

$$\Gamma_{kb} = \frac{P_{kP} \|\bar{\boldsymbol{g}}_{kb}^H \boldsymbol{f}_{kb}\|_2^2}{\|\bar{\boldsymbol{g}}_{kb}^H \boldsymbol{f}_{kb}\|_2^2 \ \sum_{k\in K} P_{kb} + \sum_{i\neq b} \ \sum_{k\in |K|} \| \bar{\boldsymbol{g}}_{kb}^H \boldsymbol{f}_{ki} \|^2 \ P_{ki} + n_{kb}^2}$$

Then substitute for U and V according to the above assumption, eq. (17.6) will be as follows,

$$(1 + \Gamma_{kb})^{-1}$$

$$= 1^{-1} - p_{kb} . \|\bar{\boldsymbol{g}}_{kb}^H . \boldsymbol{f}_{kb}\|_2^2 \, [\, p_{kb} . \|\bar{\boldsymbol{g}}_{kb}^H . \boldsymbol{f}_{kb}\|_2^2 + (\|\bar{\boldsymbol{g}}_{kb}^H \boldsymbol{f}_{kb}\|_2^2 \sum_{k\in K} P_{kb} + \sum_{i\neq b} \sum_{k\in |K|} \| \bar{\boldsymbol{g}}_{kb}^H \boldsymbol{f}_{ki} \|^2 \ P_{ki}) + n_{kb}^2 \,]^{-1}$$

$$= 1 - p_{kb} . \|\bar{\boldsymbol{g}}_{kb}^H . \boldsymbol{f}_{kb}\|_2^2 \, [\, p_{kb} . \|\bar{\boldsymbol{g}}_{kb}^H . \boldsymbol{f}_{kb}\|_2^2 + I_{kb} + n_{kb}^2 \,]^{-1} \quad \dots (17.7)$$

Which is the same expression for $MMSE_{kb}$ in Eq. (16.6); hence, the proof of this formula is complete.

Now, by comparing Eq. (17) with (16), the following expression will be as follows,

$$MMSE_{kb} = \min_{W_{kb}} MSE_{kb} = (1 + SNIR_{kb})^{-1} \tag{18}$$

To this end, the data rate's logarithmic function can be expressed as follows,

$$\log_2(1 + SINR_{kb}) = \max_{W_{mn}}\{-\log_2 MSE_{kb}\} \tag{19}$$

As a result, the primary goal has been reduced from an NP-hard optimization problem involving $SINR_{kb}$ to a more straightforward problem involving only MSE_{kb}. Additionally, by following the same procedure as described in the preceding reference, one can reduce the complexity of the objective problem and eliminate the log-term ($\log_2 MSE_{kb}$). After the real-positive-number (i.e., auxiliary factor that cannot be negative), λ_{kb} is presented, the problem ρ_1 of the data rate can be stated as,

$$\max_{P_{kb}} \sum_{i\in|b|}\sum_{k\in|\mathrm{K}|} \frac{1}{\ln 2} \max_{F_{ki}} \max_{\lambda_{ki}} \{\ln \lambda_{ki} . \lambda_{ki} MSE_{ki}\}$$

Subject to: $$C1: \quad \log_2(1 + SINR_{kb}) \geq R_{th}, \quad \forall \mathrm{b}, k \tag{20}$$

$$C2: \quad \sum_{i\in|b|}\sum_{k\in|\mathrm{K}|} P_{kb} \leq P_t$$

An iterative approach is used to determine the values of F_{kb}, and P_{kb} Individually is introduced to reduce computational complexity. The proposed algorithm updates the optimum coefficients of the equalizer, $\mathrm{W}_{kb}{}^{*(\theta)}$, the optimum value of MSE, and $MMSE_{kb}{}^{(\theta)}$ in each iteration (θ), using (14) and (15), respectively. Then, the prior maximization problem, which is expressed in Eq. (19), can be resolved using any of the optimization tools and the convex minimization formula described below,

$$\min_{P_{kb}} \sum_{i\in|b|}\sum_{\mathrm{k}\in|K|} \lambda_{kb} MSE_{kb}$$

Subject to: $$\check{C}^1: \quad \varphi_{kb} \geq \left(2^{R_{kb}{}^{Th}} - 1\right) n_{kb}{}^2, \forall\, k, \mathrm{b} \tag{21}$$

$$C^2: \quad \sum_{i\in|b|}\sum_{k\in|K|} P_{kb} \leq P_t,$$

where,

$$\varphi_{kb} = P_{kb} . \|\bar{\boldsymbol{g}}_{kb}^H . \boldsymbol{f}_{kb}\|_2^2 + \left(1 - 2^{R_{kb}{}^{Th}}\right) \|\bar{\boldsymbol{g}}_{kb}^H . \boldsymbol{f}_{kb}\|_2^2 \sum_{k\in|K|} P_{kb} + \left(1 - 2^{R_{mn}{}^{Th}}\right) \sum_{i\in|B|,\ i\neq b} \|\bar{\boldsymbol{g}}_{kb}^H . \boldsymbol{f}_{ki}\|_2^2 \sum_{k\in|K|} p_{ki}, \tag{22}$$

and the SNIR threshold is expressed as,

$$SINR^{Th} = 2^{R_{kb}{}^{Th}} - 1 \tag{23}$$

The proposed power allocation approach's pseudo-code is presented in (Algorithm I) on the next page. The numerical analysis validates the efficient performance of this algorithm, where it can assign power to each user in different beams in a few iterations.

Algorithm I Proposed MSE-DPA Framework.

Input: User's min rate: R_{kb}.

Total power transmits: P_t,
Beamspace channel matrix: $\overline{\boldsymbol{G}}_{kb}^{H}$.
Iteration Index: $\theta = 0$.

Output: power allocation vectors $\boldsymbol{p}_{kb}$,

1. Initialize the random variable of: $\boldsymbol{p}_{kb}, \boldsymbol{I}_{kb}$;
2. Update iteration index $\theta = \theta + 1$;
3. Update the optimal equalization coefficients
$$W_{\mathrm{kb}}^{*(\theta)} = \left[P_{kb}^{(\theta-1)} \cdot \|\overline{\boldsymbol{g}}_{kb}^{H} . \boldsymbol{f}_{kb}\|_2^2 + I_{kb}^{(\theta-1)} + {n_{kb}}^2\right]^{-1} \left(\sqrt{P_{\mathrm{kb}}(\theta-1)}\overline{\boldsymbol{g}}_{kb}^{H} . \boldsymbol{f}_{kb}\right)^{\mathrm{H}};$$
4. Compute the optimal of the mean-square-error
$$MMSE_{mn}{}^{(\theta)} = 1 - P_{kb}^{(\theta-1)} \cdot \|\overline{\boldsymbol{g}}_{kb}^{H} . \boldsymbol{f}_{kb}\|_2^2 \left[P_{kb}^{(\theta-1)} \cdot \|\overline{\boldsymbol{g}}_{kb}^{H} . \boldsymbol{f}_{kb}\|_2^2 + I_{kb}^{(\theta-1)} + n_{kb}^2\right]^{-1};$$
5. Compute the value of constraint 1
$$\varphi_{kb}^{(\theta)} = P_{kb}^{(\theta)} \cdot \|\overline{\boldsymbol{g}}_{kb}^{H} . \boldsymbol{f}_{kb}\|_2^2 + \left(1 - 2^{{R_{kb}}^{Th}}\right) \|\overline{\boldsymbol{g}}_{kb}^{H} . \boldsymbol{f}_{kb}\|_2^2 \sum_{j\in|S_{\mathrm{group}}|} p_{mj}^{(\theta)} + \left(1 - 2^{{R_{kb}}^{Th}}\right) \sum_{i\in|B|, i\neq b} \|\overline{\boldsymbol{g}}_{kb}^{H} . \boldsymbol{f}_{ki}\|_2^2 \sum_{k\in|K|} P_{ki}^{(\theta)};$$
6. Solve the convex minimization problem via the CVX tool, a package for specifying and solving convex programs [35], [36]:
$$\text{Problem: } \min_{P_{kb}(\theta)} \sum_{t\in|b|} \sum_{k\in|K|} {\lambda_{kb}}^{(\theta)} MSE_{kb}{}^{(\theta)}$$
$$C^1: {\varphi_{kb}}^{(\theta)} \geq \left(2^{R_{kb}^{Th}} - 1\right) {n_{kb}}^2, \forall k, b$$
$$C^2: \sum_{\mathbf{i}\in|b|} \sum_{k\in|K|} {P_{kb}}^{(\theta)} \leq P_t$$
7. Check for convergence; if not, go back to step 2 in the next iteration.
Else,
return Power allocation vectors: $\boldsymbol{p}_{kb}$.
8. **End Algorithm I**

6. NUMERICAL AND SIMULATION RESULTS

This section discusses the EE performance of the BS-MIMO-NOMA at mm-Wave with the power allocation technique. The system information illustrated in Table 1 with values for the corresponding parameters is considered. The AP is assumed to have complete beamspace channel information for all users. In addition to our proposed approach, we compare it to three different baselines, which are as follows,

1. Traditional MIMO scheme with fully-digital beamforming.
2. Traditional MIMO-OMA scheme.
3. Traditional Beamspace-OMA scheme.

Table 1: Simulation system setting.

Parameter	setting
Total transmitted power	$P_t =$ 16 dBm
Power losses in RF-Chains	$P^{RF} =$ 25 dBm
Power losses in baseband network	$P^{BB} =$ 23 dBm
Power losses in the switch network	$P^{SN} =$ 1.6 dBm
channel model	The geometric Saleh-Valenzuela [3].
channel-path number	3 – 1 for LoS and 2 for NLoS
Carrier frequency	32 GHz
BS antenna number N	256 elements
Users number K	[5 - 55] users
Transceivers' chain number	$N_{Rf} =$ { N, K } for the benchmarks $N_{Rf} \leq K$ for the proposed algorithm

The metric that is considered in this section is the energy efficiency, i.e., EE for the proposed scheme in terms of Bits/Hz/Joule, which can be determined as follows [18],

$$\xi_{Energy} = \frac{R_{sum-rate}}{consumed\ eneregy} \tag{23}$$

Where, $R_{sum-rate} = \sum_{i \in |b|} \sum_{k \in |K|} \log_2(1 + \Gamma_{ki}) \quad bits/sec/Hz$ and,

$$consumed\ eneregy = P_t + P^{RF} + P^{BB} + P^{SN} \tag{24}$$

Figure 4 shows that our proposed algorithm may attain an acceptable EE value after only 3-5 iterations. Additionally, after ten iterations, the maximum increase in EE can be achieved.

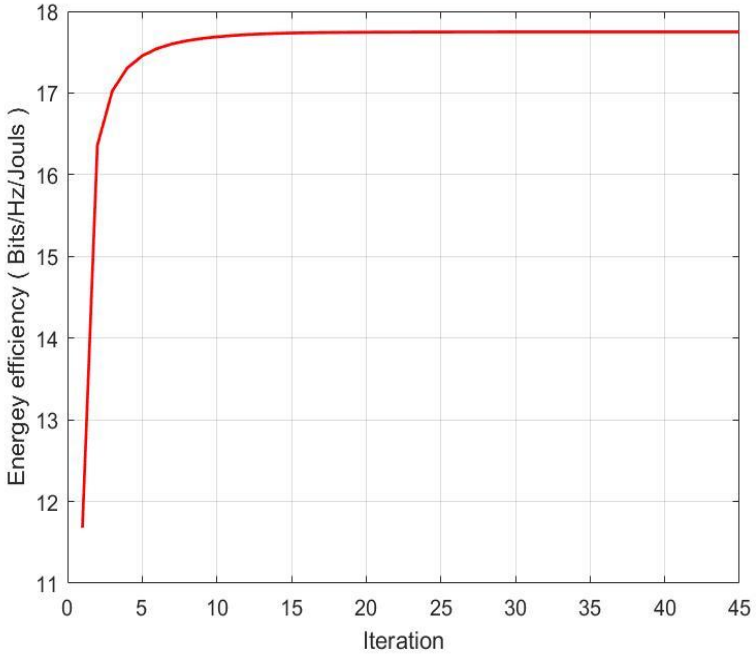

Figure 4. Energy Efficiency vs Number of Iterations.

Following that, Figure 5 shows a clear superiority of the proposed BS-MIMO-NOMA over the other MIMO systems in terms of EE performance as a function of the served users' number. For 30 users, the proposed approach outperforms the traditional MIMO-OMA scheme by approximately 11%, the traditional beamspace-OMA scheme by approximately 32.5%, and the classic MIMO scheme by approximately five times. This superiority is so clear that it increases with the increase of users. On the other hand, when the EE is plotted concerning transmit power, as shown in figure 6, the proposed approach outperforms the other schemes.

For a transmit power of 15 dBm, the proposed BS-MIMO-NOMA has a superiority percentage of approximately 11.5% greater than MIMO-OMA, approximately 27% better than beamspace-MIMO OMA, and approximately 85% greater than fully-digital MIMO.

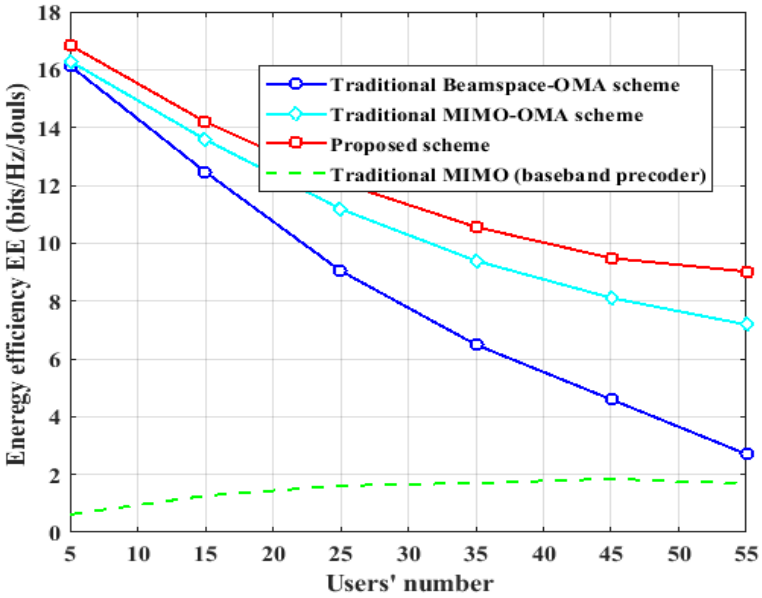

Figure 5. Energy efficiency vs users' number under nine dBm.

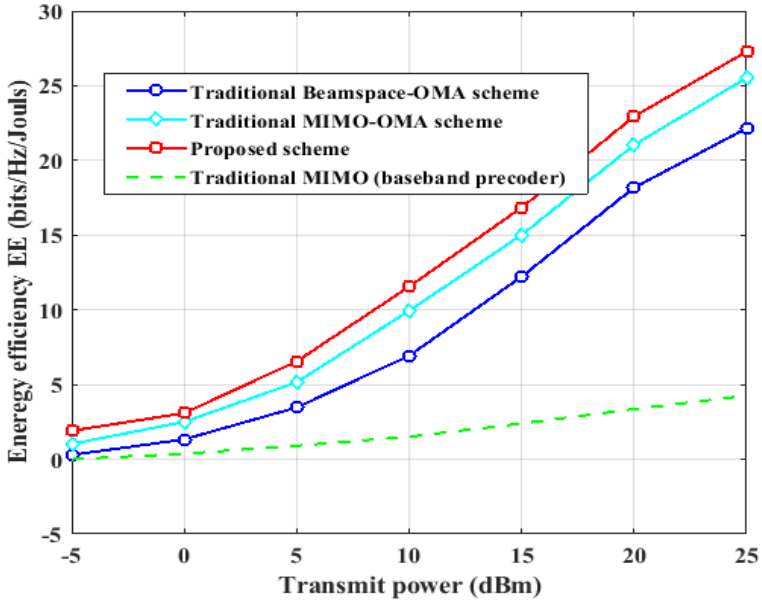

Figure 6. Energy efficiency vs Transmit Power for 30 users.

7. CONCLUSION

This work aims to investigate the topic of data-throughput enhancement for the BS-MIMO-NOMA approach in mm-wave wireless communications systems under two constraints, the budget of total power and the QoS of each user. A simple iterative scheme for the dynamic power allocation algorithm is considered in the proposed model, where the MSE approach is employed to decrease the complexity of the non-convex problem in the proposed beamforming algorithm. A near-optimum solution was obtained with a few iterations. The proposed model achieves a higher EE performance than the traditional schemes that do not apply the beamspace concept for the MIMO-NOMA technology.

REFERENCES

[1] S. Mattisson, "An Overview of 5G Requirements and Future Wireless Networks: Accommodating Scaling Technology," *IEEE Solid-State Circuits Mag.*, vol. 10, no. 3, pp. 54–60, 2018, doi: 10.1109/MSSC.2018.2844606.

[2] S. Rajoria, A. Trivedi, and W. W. Godfrey, "A comprehensive survey: Small cell meets massive MIMO," *Phys. Commun.*, vol. 26, pp. 40–49, 2018, doi: 10.1016/j.phycom.2017.11.004.

[3] J. Brady, N. Behdad, and A. M. Sayeed, "Beamspace MIMO for millimeter-wave communications: System architecture, modeling, analysis, and measurements," *IEEE Trans. Antennas Propag.*, vol. 61, no. 7, pp. 3814–3827, Jul. 2013, doi: 10.1109/TAP.2013.2254442.

[4] X. Gao, L. Dai, S. Han, I. Chih-Lin, and R. W. Heath, "Energy-Efficient Hybrid Analog and Digital Precoding for MmWave MIMO Systems with Large Antenna Arrays," *IEEE J. Sel. Areas Commun.*, vol. 34, no. 4, pp. 998–1009, 2016, doi: 10.1109/JSAC.2016.2549418.

[5] Y. R. Lee, W. S. Lee, J. S. Jung, C. Y. Park, Y. H. You, and H. K. Song, "Hybrid Beamforming with Reduced RF Chain Based on PZF and PD-NOMA in mmWave Massive MIMO Systems," *IEEE Access*, vol. 9, pp. 60695–60703, 2021, doi: 10.1109/ACCESS.2021.3073502.

[6] R. Mendez-Rial, C. Rusu, N. Gonzalez-Prelcic, A. Alkhateeb, and R. W. Heath, "Hybrid MIMO Architectures for Millimeter Wave Communications: Phase Shifters or Switches?," *IEEE Access*, vol. 4, no. c, pp. 247–267, 2016, doi: 10.1109/ACCESS.2015.2514261.

[7] T. Gong, N. Shlezinger, S. S. Ioushua, M. Namer, Z. Yang, and Y. C. Eldar, "RF Chain Reduction for MIMO Systems: A Hardware Prototype," *IEEE Syst. J.*, vol. 14, no. 4, pp. 5296–5307, 2020, doi: 10.1109/JSYST.2020.2975653.

[8] P. V. Amadori and C. Masouros, "Low RF-Complexity Millimeter-Wave Beamspace-MIMO Systems by Beam Selection," *IEEE Trans. Commun.*, vol. 63, no. 6, pp. 2212–2223, Jun. 2015, doi: 10.1109/TCOMM.2015.2431266.

[9] J. Choi, J. Sung, B. L. Evans, and A. Gatherer, "ANTENNA SELECTION FOR LARGE-SCALE MIMO SYSTEMS WITH LOW-RESOLUTION ADCS," *IEEE ICASSP 2018*, pp. 3594–3598, 2018.

[10] X. Gao, L. Dai, Z. Chen, Z. Wang, and Z. Zhang, "Near-Optimal Beam Selection for Beamspace MmWave Massive MIMO Systems," *IEEE Commun. Lett.*, vol. 20, no. 5, pp. 1054–1057, May 2016, doi: 10.1109/LCOMM.2016.2544937.

[11] A. Liu and V. Lau, "Phase only RF precoding for massive MIMO systems with limited RF chains," *IEEE Trans. Signal Process.*, vol. 62, no. 17, pp. 4505–4515, 2014, doi: 10.1109/TSP.2014.2337840.

[12] K. H. Yuya S., Y. Kishiyama, Anass Benjebbour, T. Nakamura, Anxin Li, "Non-Orthogonal Multiple Access (NOMA) for Cellular Future Radio Access," *IEEE VTC2013-Spring*, 2013.

[13] L. Dai, B. Wang, Y. Yuan, S. Han, I. Chih-Lin, and Z. Wang, "Non-orthogonal multiple access for 5G: solutions, challenges, opportunities, and future research trends," *IEEE Commun. Mag.*, vol. 53, no. 9, pp. 74–81, 2015.

[14] P. Liu, Y. Li, W. Cheng, W. Zhang, and X. Gao, "Energy-efficient power allocation for millimeter wave beamspace MIMO-NOMA systems," *IEEE Access*, vol. 7, pp. 114582–114592, 2019, doi: 10.1109/ACCESS.2019.2935495.

[15] J. Zeng *et al.*, "Investigation on Evolving Single-Carrier NOMA into Multi-Carrier NOMA in 5G," *IEEE Access*, vol. 6, no. c, pp. 48268–48288, 2018, doi: 10.1109/ACCESS.2018.2868093.

[16] F. Lu, M. Xu, L. Cheng, J. Wang, and G. K. Chang, "Power-Division Non-Orthogonal Multiple Access (NOMA) in Flexible Optical Access with Synchronized Downlink/Asynchronous Uplink," *J. Light. Technol.*, vol. 35, no. 19, pp. 4145–4152, 2017, doi: 10.1109/JLT.2017.2721955.

[17] A. Kassir, R. A. Dziyauddin, H. M. Kaidi, and M. A. Mohd Izhar, "Power Domain Non Orthogonal Multiple Access: A Review," *2018 2nd Int. Conf. Telemat. Futur. Gener. Networks, TAFGEN 2018*, pp. 66–71, 2018, doi: 10.1109/TAFGEN.2018.8580477.

[18] I. Hburi, H. F. Khazaal, N. M. Mohson, and T. Abood, "MISO-NOMA Enabled mm-Wave: Sustainable Energy Paradigm for Large Scale Antenna Systems," in *2021 International Conference on Advanced Computer Applications (ACA)*, Jul. 2021, pp. 45–50. doi: 10.1109/ACA52198.2021.9626818.

[19] S. M. R. Islam, N. Avazov, O. A. Dobre, and K. S. Kwak, "Power-Domain Non-Orthogonal Multiple Access (NOMA) in 5G Systems: Potentials and Challenges," *IEEE Commun. Surv. Tutorials*, vol. 19, no. 2, pp. 721–742, 2017, doi: 10.1109/COMST.2016.2621116.

[20] B. Wang, L. Dai, X. Gao, and L. Hanzo, "Beamspace MIMO-NOMA for millimeter-wave communications using lens antenna arrays," *IEEE Veh. Technol. Conf.*, vol. 2017-Septe, pp. 1–5, 2017, doi: 10.1109/VTCFall.2017.8288345.

[21] S. M. Nimmagadda, "A New HBS Model in Millimeter-Wave Beamspace MIMO-NOMA Systems Using Alternative Grey Wolf with Beetle Swarm Optimization," *Wirel. Pers. Commun.*, vol. 120, no. 3, pp. 2135–2159, Oct. 2021, doi: 10.1007/s11277-021-08696-6.

[22] M. Shili, M. Hajjaj, and M. L. Ammari, "Power allocation with QoS satisfaction in mmWave beamspace MIMO-NOMA," *IET Commun.*, vol. 16, no. January, pp. 1–8, Jan. 2021, doi: 10.1049/cmu2.12325.

[23] D. S and M. L. M. J, "Energy Efficient Power Allocation Framework for downlink MIMO-NOMA Heterogeneous IoT network: Non-Deep Learning and Deep Learning Approaches," 2021.

[24] J. D. Parsons, *The Mobile Radio Propagation Channel*. 2000. doi: 10.1002/0470841524.

[25] A. A. M. Saleh and R. A. Valenzuela, "A Statistical Model for Indoor Multipath Propagation," *IEEE J. Sel. Areas Commun.*, vol. 5, no. 2, pp. 128–137, 1987, doi: 10.1109/JSAC.1987.1146527.

[26] Y. Zeng and R. Zhang, "Millimeter wave MIMO with lens antenna array: A new path division multiplexing paradigm," *IEEE Trans. Commun.*, vol. 64, no. 4, pp. 1557–1571, 2016, doi: 10.1109/TCOMM.2016.2533490.

[27] A. Sayeed and J. Brady, "Beamspace MIMO for high-dimensional multiuser communication at millimeter-wave frequencies," *GLOBECOM - IEEE Glob. Telecommun. Conf.*, pp. 3679–3684, Dec. 2013, doi: 10.1109/GLOCOM.2013.6831645.

[28] B. Wang, L. Dai, Z. Wang, N. Ge, and S. Zhou, "Spectrum and Energy-Efficient Beamspace MIMO-NOMA for Millimeter-Wave Communications Using Lens Antenna Array," *IEEE J. Sel. Areas Commun.*, vol. 35, no. 10, pp. 2370–2382, 2017, doi: 10.1109/JSAC.2017.2725878.

[29] I. S. Hburi, "Asymptotic Performance of Multiuser Massive MIMO systems," Brunel University, London, 2017.

[30] Z. Q. Luo and W. Yu, "An introduction to convex optimization for communications and signal processing," *IEEE J. Sel. Areas Commun.*, vol. 24, no. 8, pp. 1426–1438, 2006, doi: 10.1109/JSAC.2006.879347.

[31] Z. Q. Luo and S. Zhang, "Dynamic spectrum management: Complexity and duality," *IEEE J. Sel. Top. Signal Process.*, vol. 2, no. 1, pp. 57–73, 2008, doi: 10.1109/JSTSP.2007.914876.

[32] Q. Zhang, Q. Li, and J. Qin, "Robust Beamforming for Nonorthogonal Multiple-Access Systems in MISO Channels," *IEEE Trans. Veh. Technol.*, vol. 65, no. 12, pp. 10231–10236, 2016, doi: 10.1109/TVT.2016.2547998.

[33] William H. Press, S. A. Teukolsky, W. T. Vetterling, and B. P. Flannery, *NUMERICAL RECIPES The Art of Scientific Computing*, Third Edit. New York: Cambridge University Press, 2007.

[34] J. Sherman and W. J. Morrison, "Adjustment of an Inverse Matrix Corresponding to a Change in One Element of a Given Matrix," *Ann. Math. Stat.*, vol. 21, no. 1, pp. 124–127, Mar. 1950, doi: 10.1214/aoms/1177729893.

[35] Michael Grant and Stephen Boyd, "CVX: Matlab software for disciplined convex programming, version 2.0 beta."

[36] Michael Grant and Stephen Boyd, "Graph implementations for nonsmooth convex programs, Recent Advances in Learning and Control (a tribute to M. Vidyasagar)," *Springer*, 2008.